



Open Archive Toulouse Archive Ouverte (OATAO)

OATAO is an open access repository that collects the work of some Toulouse researchers and makes it freely available over the web where possible.

This is an author's version published in: <https://oatao.univ-toulouse.fr/24076>

Official URL : <https://doi.org/10.23919/EuCAP.2017.7928426>

To cite this version :

Grzeskowiak, Marjorie and Diet, Antoine and Benamara, Megdouda and Protat, Stéphane and Conessa, Christophe and Biancheri-Astier, Marc and De Oliveira Alves, Francisco and Le Bihan, Yann and Lissorgues, Gaëlle Coaxially distributed diameter sub-coil twisted loop antenna in HF RFID. (2017) In: 2017 11th European Conference on Antennas and Propagation (EUCAP), 19 March 2017 - 24 March 2017 (Paris, France).

Any correspondence concerning this service should be sent to the repository administrator:

tech-oatao@listes-diff.inp-toulouse.fr

Coaxially Distributed Diameter sub-Coil Twisted Loop Antenna in HF RFID

Marjorie Grzeskowiak¹, Antoine Diet², Megdouda Benamara¹, Stéphane Protat¹, Christophe Conessa², Marc Biancheri-Astier³, Franciso de Oliveira Alves², Yann Le Bihan², Gaelle Lissorgues¹

¹ (ESYCOM EA 2552) : UPEM, ESIEE-Paris, CNAM, 77454 Marne-la-Vallée, France, marjorie.grzeskowiak-lucas@u-pem.fr

² (GeePs UMR 8507): Univ. Paris-Saclay, 91192 Gif Sur Yvette, France. antoine.diet@geeps.centralesupelec.fr

³ (GEOPS/GPIS UMR 8148): Univ. Paris-Saclay, 91405 Orsay, France, marc.biancheri-astier@u-psud.fr

Abstract— This paper proposes an HF (High Frequency) transmitting coil less sensitive to the angular and position misalignments of the small receiving coil. The DDC (Distributed Diameter Coil) shape and TLA (Twisted Loop Antenna) allow respectively minimizing the disturbance of the magnetic link due to the lateral misalignment and the relative tilting direction of the transmitting coil to the receiving coil. The magnetic coupling link obtained from DDC TLA coils is illustrated by comparison with conventional TLA in the case of HF RFID.

Index Terms— HF RFID, coil, near field, magnetic coupling.

I. INTRODUCTION

In RFID (IDentification by RF communication) and HF WPT (Wireless Power Transfer), higher magnetic flux, proportional to induced current on small receiving coil, provides wider useful operating plane to activate a receiving system [1]. In RFID applications, the transponders responses are detected by the interrogator as load modulations of the induced field, while for the WPT applications [2], the budget link is determined versus the energy efficiency [3]. In the both cases, stronger H-field enhances the power for the receiving hardware at the required read-out distance. With the miniaturization of receiving coils [4], it is a challenge to power a receiving system whose effective area is relatively smaller in comparison with the surface of the transmitting coil. These RFID and WPT applications would like to activate area of receiving systems whatever their angular and position misalignments versus the transmitting coil [5],[6]. The objectives in this paper are two-fold: sizes of the receiving coil in comparison with the transmitting coil, and angular/position misalignments. Design of a planar transmitting coil allowing the modification of the magnetic field (intensity and orientation) could be suitable for a HF RFID reader antenna. This later is installed under a movable tray, on which are placed tagged arbitrary oriented objects.

To enhance the magnetic coupling with a small and arbitrary oriented receiving coil, DDC (Distributed Diameter Coil) shape [7] that favors the magnetic link with a small misaligned coil, is inserted in the TLA (Twisted

Loop Antenna) [8]. The goal is to improve the magnetic coupling when the coil is coplanar to the axis of the TLA plane.

First, the authors describe the studied transmitting coils. In a second part, the performance of the system in magnetic coupling with a small receiving coil is presented: the measured values of mutual inductance between the transmitting and receiving coils are compared with the simulated one as function of both position misalignment and distance for parallel and normal positions of the receiving coils over transmitting area. In the last part, RFID set-ups illustrate the activate area of the receiving coils with the detection distances for two sizes of tags and for the both orientations.

II. THE DDC TLA STRUCTURE

The TLA [8] and DDC [7] are mixed to enhance respectively the magnetic field coupling whatever the orientation and position of the receiving coil versus the transmitting coil. In the TLA structure, the two coils are complementary and for each sub-coil, the direction of the current is assumed to be equal in all the turns.

In the conventional coil, the sub-coil diameter of the transmitter antenna is 4.5 wider than the receiving coil, while in the second and third structures, in keeping constant the self-inductance of the DDC TLA coil, a second and third sub-coil are respectively added. The third sub-coil presents a diameter comparable to the receiving coil, while the second one is intermediate between the upper and downer diameters. It should be noted that the coupling with the receiving coil, was calculated without matching the coils to source and load impedances. The S-parameter won't be done in order to appreciate the effect of variations in magnetic flux on the RFID and WPT systems.

The transmitting coils are designed with the same inductance value L_1 and the quality factor Q is in the same order to generate an equivalent magnetic energy. Three combinations of turns with diameters in centimeter d_1 , d_2 and d_3 , are evaluated empirically in neglecting the mutual coupling between each of sub-coils and in summing the

inductance $L_{d_i}^N$, expressed in nH, corresponding to each sub-coil of diameter d_i of N_i turns and used in Ib Technology UK [9].

$$L_{d_i}^N = 2\pi d_i \ln\left(\frac{\pi d_i}{d_w}\right) N^{1.9}; L_1 = L_{d_1}^{N_1} + L_{d_2}^{N_2} + L_{d_3}^{N_3} \quad (1)$$

If we consider the mutual inductance between pair of coaxial sub-coils, we can calculate the mutual inductance $M_{a,b}$ for N_a and N_b turn numbers of the considered sub-coils.

In the case of perfect alignment of coplanar loops, the mutual inductance $M_{a,b}$ [4] is

$$M_{a,b} = N_a N_b \mu_0 \sqrt{ab} \left[\left(\frac{2}{K} - K \right) K(K) - \frac{2}{K} E(K) \right] \quad (2)$$

Where $K = \left(\frac{4ab}{(a+b)^2} \right)^{1/2}$ (3)

a and b are the radii of the coaxial sub-coils, $K(K)$ and $E(K)$ respectively the complete elliptic integrals of the first and second kind. N_a and N_b are the turn numbers of the considered sub-coils diameter.

The value of the self-inductance of the empirical inductance L_{1E} is calculated in considering (1) and (2) with enameled copper wire having an external diameter of 0.022 cm, whose enamel thickness is known to be around 5 to 50 μm . The value of the copper wire diameter is comprised between 0.012 cm and 0.021 cm, and the L_{1E} respectively between $L_{1E\text{min}}$ and $L_{1E\text{max}}$.

The simulated inductance L_{1s} is carried out using HFSS [HFSS] (High Frequency Structure Simulator [10]). The metalized wire of the coil is replaced by copper boundaries on strip of $1\mu\text{m}$ width without thickness, to reduce the time process. The measured inductance L_{1M} is measured on a Rhode Schwarz ZNB8 VNA. The diameters are set in the fabricated 3-D printing base, represented in figure 1.

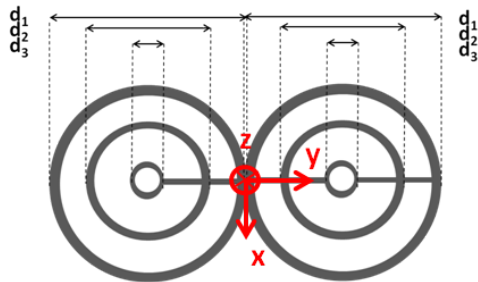


Fig. 1. Layout for 3D fabricated plastic base ($d_1=4.5\text{cm}$, $d_2=2.5\text{cm}$, $d_3=0.45\text{cm}$)

The external diameters d_1 , d_2 and d_3 are respectively set to 4.5 cm, 2.5 cm and 0.45 cm: the A ($3d_1-0d_2-0d_3$) coil, with each number corresponding to the number of turns of the associated diameter, correspond to the conventional coil in [2] and B ($2d_1-3d_2-0d_3$), and E ($1d_1-3d_2-7d_3$) coils to evaluate the impact on the DDC profile. The width and the depth of the slot are respectively equal to 2mm and 5 mm.

The empirical value of the DDC TLA inductance is reported and compared with the simulated and the measured

ones in the table 1. We consider the internal diameters of the coils to calculate the self-inductances. Electrical characteristics (empirical, simulated and measured) of the DDC TLA coils.

TABLE I. ELECTRICAL CHARACTERISTICS (EMPIRICAL, SIMULATED AND MEASURED) OF THE DDC TLA COILS

DDC TLA	A	B	E
$L_{1E}(\mu\text{H})$ min	2.068	2.126	1.6658
$L_{1E}(\mu\text{H})$ max	2.19	2.248	1.781
$L_{1S}(\mu\text{H})$	1.94	1.98	1.77
$R_{1S}(\Omega)$	2.2	2.2	3.4
$L_{1M}(\mu\text{H})$	2.38	2.79	2.26
$R_{1M}(\Omega)$	3.1	4.4	3.4

In table I, empirical, simulated and measured inductances for each coil are compared, and show an important difference with the measured one, that can be explained by length of wires to join the sub-coils and to feed the coils by SMA connector in realized structure. For the practical one, enamel thickness, due to uncertainty, doesn't correspond to the width of the strip. We can precise the neglecting of the conductor losses because of the null thickness of the strip.

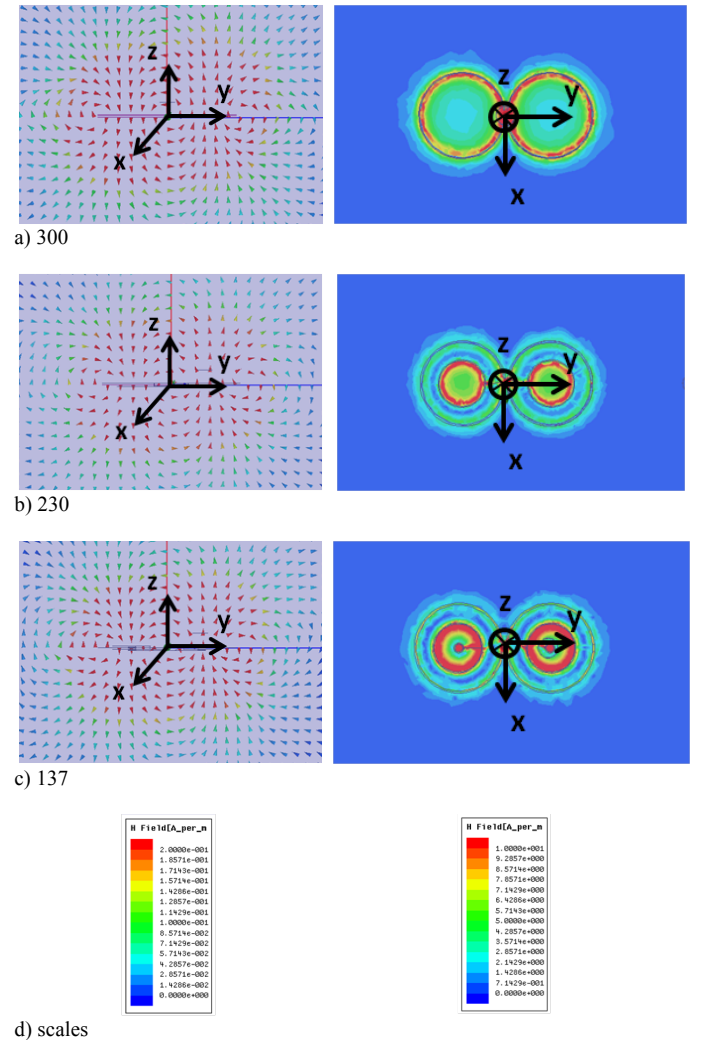


Fig. 2. Displaying of the magnetic field

The electromagnetic simulation has been implemented with PEC strip, the aim is not accuracy but to understand the trend of variation of magnetic coupling with changing physical coil parameter-

The magnetic field is displayed (Fig.2) in the (y0z) plane on the left side for the H-field vector and in the (x0y) plane for the H-field magnitude for each DDC TLA structure. While the orientation of the H-field vector seems similar for each structure, the distribution of the magnitude is different and the contribution of the different diameter can be observed.

The displaying is useful to illustrate the magnetic field but to see clearly the magnetic coupling with a small receiving coil, and compare the structure between themselves, it is necessary to use a quantified parameter, as the mutual inductance.

III. MUTUAL INDUCTANCE

The above studies have been tested using FEM (Finite Element Method) with the commercial software Ansys HFSS. The comparison of the different DDC TLA structures versus the inductive coupling between the coils, is possible on the simulated software, and compared with the measured ones, thanks to the experimental setup defined in figure 3. The simulation was performed with the assumption that the coils aren't matched to the 50Ω ports. The simulated and measured values of the DDC coil are reported on the table 1, the experimental spiral loop presents an impedance equal to $10+j311$ ($L_C=3.6 \mu\text{H}$), while in simulation it is calculated to $0.31+j2.67$ ($L_C=0.0313 \mu\text{H}$). The structure of receiving coil is different: it is a spiral coil on both sides of the FR4 substrate in the experimental case while it corresponds to a single coil in the simulated study. In this setup, DX relative location of the DDC TLA transmitting coil to the receiving coil and DZ height are varied in VM (and HM) modes, when the TAGs surface is perpendicular (and parallel) to this one of the DDC TLA surface. The center of the coil tested is the origin. DY will not be used and only positive values for DX are considered for reasons of symmetry. We report, at the height $DZ=10\text{mm}$, the mutual inductance M versus DY variation in simulation (Fig.4) and in measure (Fig.5) and the Figures of Merit (Fig.6 and Fig.7), to evaluate the improvement of the Coupling Capability (2) and the peak of mutual inductance. The CC FoM, by means of the integral of the mutual inductance $M(y)$ absolute value along the dY axis (Fig.1), allows to estimate the detection of tag whatever its orientation, while the peak of mutual inductance characterizes a maximum of detection range at one point. The improvement of these both parameters can permit to check the best structure to feed a tag by magnetic coupling. The aim is to increase the distance and the area ranges.

$$CC = \int_{Y_1}^{Y_2} |M(y)| dy \quad (2)$$

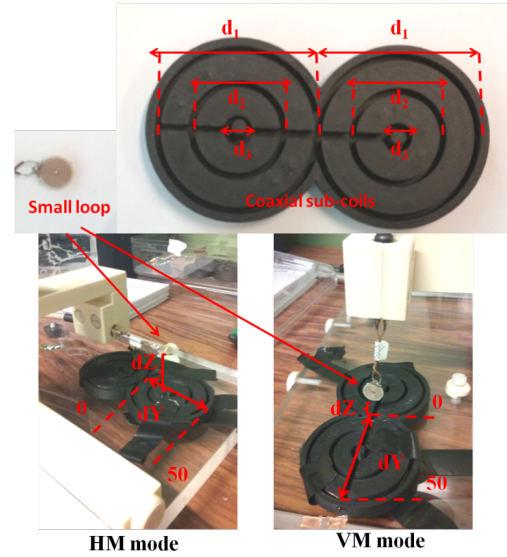


Fig. 3. Experimental setup with DX and DZ variation in millimeter

Fig.4 and Fig.5 depict respectively the mutual inductance M between the DDC TLA and the small coils as a function of the DY misalignment for the simulated and measured results.

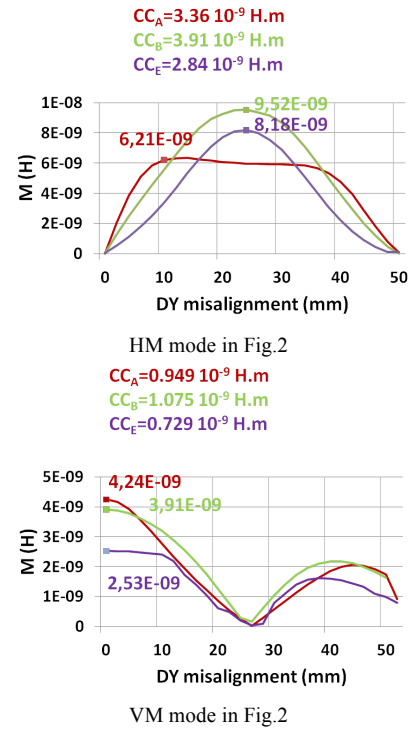


Fig. 4. Simulated mutual inductance M versus lateral misalignment DY at height $DZ=10 \text{ mm}$

The simulated and measured values are different because the structure of receiving coil is different, but the behaviour of mutual inductance is the same one and confirms the enhancement of the B structure in HM mode, and the

optimisation of the CC parameter in VM mode for the B structure.

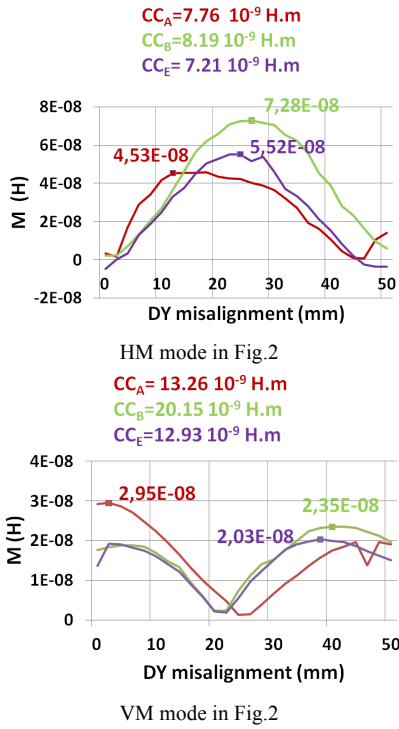


Fig. 5. Measured mutual inductance M versus lateral misalignment DY at height $DZ=10$ mm

The comparison of the different DDC TLA structures as efficient WPT transmitting coils, is possible with a parametric study on the simulated software versus the height $d=DZ$ for each HM and VM mode (Fig.6). We have reported the mutual inductance M , the coupling is less sensitive to vertical displacement for B coil that keeps a greater value M than the other structures in HM mode.

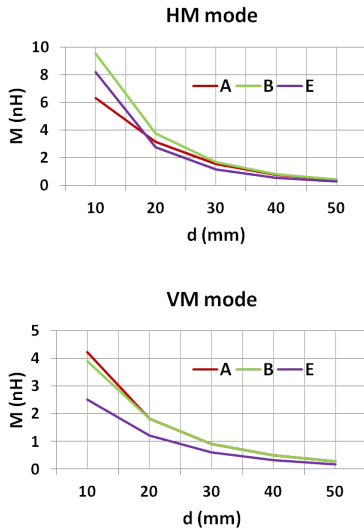


Fig. 6. M versus d (from 10mm to 50 mm by 10mm step) in HM and VM modes

Each On-center structure is loaded with a capacitor $C_{//}$ to resonate around 13.56MHz in parallel with a resistance $R_{//}$ to equalize the quality factor Q_{BTS1} of the DDC On-center structure around 25. In order to analyze the frequency impact, $dB_{20}(\text{mag}Z_{12})$ is reported versus the misalignment and the Z bandwidth is calculated in 3 dB frequency-band. Weaker coupling between the transmitting coil and small receiving coil could result in a frequency shift (less than 1%) of the trans-impedance. The bandwidth of the trans-impedance of the links at the resonant frequency is slightly affected by the lateral misalignment. However, table II shows that the Z bandwidth seems constant with the different DDC TLA. Furthermore, larger the value of M , higher will be the efficiency, with a kept constant bandwidth frequency and negligible frequency shift.

TABLE II. ELECTRICAL CHARACTERISTICS OF THE DDC ON-CENTER ($C_{//}$, $R_{//}$, Q) AND MINIMUM AND MAXIMUM VALUES OF FREQUENCY BANDWIDTH OF THE TRANS-IMPEDANCE VERSUS THE DY MISALIGNMENT

DDC TLA	A	B	E
$C_{//}$ (pF)	70	64	78
$Q_{BTS1} = \frac{f_r}{\Delta F}$	79.8	79.5	43.3
$R_{//}$ (k Ω)	6500	6500	9000
$Q_{BTS2} = \frac{f_r}{\Delta F}$	25.6	25.03	25.52
Z BP min (MHz)	490	500	520
Z BP max (MHz)	530	520	530
$Q_{BTM1} = \frac{f_r}{\Delta F}$	32	25	35
Q_{BTM2}	25	25	25

The measured quality factor (Q_{BTM1}) is reported in table II. The values of Q_{BTM} are impacted by the inter-turns capacitive effects in HF and by the wire losses whose length that are respectively 40.52 (A), 48.69 (B), and 40.69 (E) cm: a parallel resistance is added on the DDC TLA to equalize the quality factor Q_{BTM2} after tuning.

To validate the improvement of the mutual inductance with a very weak frequency shift in keeping constant the frequency bandwidth, we realize RFID detection as used case with the DDC On center and two types of tag.

IV. RFID VOLUME DETECTION

RFID read-out distance illustrates the impact of the different DDC TLA on the power transfer efficiency and characterizes the magnetic coupling. The comparison concerns structures with almost the same values for L_1 and Q (tables I and II). The RFID tags have different diameters (2cm for Mifare chip (Fig.8)[11] and 0.7cm for NXP chip (Fig.9) [12]) and are in the same order than respectively the intermediate ($d_2=2.5$ cm in Fig.1) and small sub-coils diameter ($d_3=0.45$ cm in Fig.1).

The tag is placed in an area where the read-out distance is optimal, i.e. above the center of the sub-coils in HM mode and in the center of the DDC TLA antenna in VM mode.

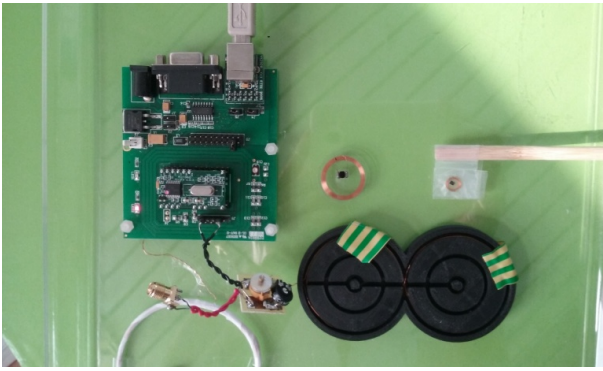


Fig. 7. RFID experimental setup

The B DDC TLA presents an improvement of operating read-out distance with each tag in HM and VM modes. The enhancement in HM mode with the smaller tag in comparison with the wider one for the B structure could be explained by a supposed more efficient chip with the NXP technology.

In VM and HM modes, we can notice an enhancement of performances of the E structure for the smaller tag in comparison with the wider one while the inverse phenomenon is observed for the A structure. This improvement is probably due to the similar geometry between the sub-coil and the tag diameters. Parametric studies on the tag diameter should be done to confirm the previous assumption and to explain the improvement of the B structure with wider (and supposed less efficient) tag in VM mode.

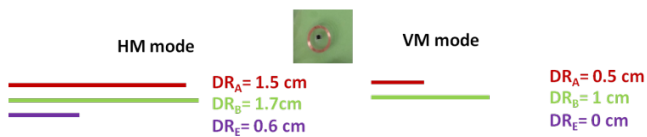


Fig. 8. Detection Range in HM and VM modes for 2cm diameter tag [11]

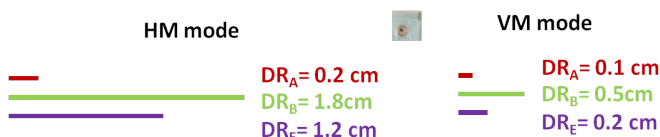


Fig. 9 : Detection Range in HM and VM modes for 0.7 cm diameter tag [12]

V. CONCLUSION

Symmetrical sub-coil DDC TLA applied to WPT and RFID systems allow changing of the distribution and orientation of magnetic field. The studied parameters to optimize the read-out distance whatever the orientation of the receiving coil over a large area are respectively the mutual inductance M and the coupling capability CC , with a receiving coil surface corresponding to one-fortieth of the transmitting coil. This design approach results in an enhancement of the mutual inductance and of the coupling capability, while achieving weak resonant frequency shift

(less than 1% at 10mm above the transmitting coil) and keeping constant the trans-impedance bandwidth frequency versus the relative position of the receiving coil. The effectiveness of the optimized design is proved by the results of RFID detection range in the close regions of antenna. This study could be applied to free-positioning small RFID tags placed on arbitrary oriented objects for instance on a movable tray. A parametric study on the diameter of the receiving coil could be realized to compare the impact on the mutual inductance and coupling capability, and RFID detection would be measured with the same RFID chip to validate the enhancement of the selected coupling parameters M and CC . Future work will consider studies on asymmetrical DDC sub-coil shapes for finding critical parameters impacting the efficiency of the magnetic coupling.

ACKNOWLEDGMENT

This work was supported by the Université Paris-Est thought a visiting period of 6 months accorded to M.Grzeskowiak in the laboratory GEEPS (CNRS, CentraleSupélec, Paris-Sud, UPMC).

REFERENCES

- [1] K. Finkenseller, RFID Handbook: Radio-Frequency, Identification Fundamentals and Application, 2nd edition, Wiley, 2003.
- [2] J. D. Heebl, E. M. Thomas, R. P. Penno, A. Grbic, Comprehensive Analysis and Measurement of Frequency-Tuned and Impedance-Tuned Wireless Non-Radiative Power-Transfer Systems, IEEE Antennas and Propagation Magazine, Vol.56, No.4, August 2014, pp. 44-60.
- [3] A. Rajagopalan, A. K. RamRakhyani, D. Schurig, G. Lazzi, Improving Power Transfer Efficiency of a Short-Range Telemetry System Using Compact Metamaterials, IEEE Transactions on Microwave Theory and Techniques, Vol.62, No.4. April 2014, pp. 947-955.
- [4] C.M. Zierhofer, E.S. Hochmair, Geometric approach for coupling enhancement of magnetically coupled coils, IEEE Transactions on biomedical engineering, Vol.43, No.7, July 1996, pp.708-714.
- [5] K. Fotopoulou, B. W. Flynn, Wireless Power Transfer in Loosely Coupled Links: Coil Misalignment Model, IEEE Transactions on magnetics, Vol.47, No.2, February 2011, pp. 416-430.
- [6] D.H. Kim, J. Kim, Y.J. Park, Free-positioning Wireless Power Transfer using multiple coupling coils in a transmitter, IEEE Antennas and Propagation in Wireless Communications (AWPC), Septembre 2015,
- [7] A. Diet, M. Grzeskowiak, Y. Le Bihan, M. Biancheri-Astier, M. Lahrar, C. Conessa, M. Benamara, G. Lissorgues, F. Alves, Improvement of RFID HF tags detection with a distributed diameter coil, Antennas and Wireless Propagation Letters, in press
- [8] M. Benamara, M. Grzeskowiak, A. Diet, G. Lissorgues, C. Conessa, S. Protat, Y. Le Bihan, Twisted Loop Antenna for HF RFID detection surface, EuCAP, Avril 2016, Davos, Suisse
- [9] Ib technology application note for 13,56 MHZ RFID reader antenna design http://www.ibtechnology.co.uk/pdf/antenna_1356.PDF
- [10] <http://www.ansys.com/Products/Simulation+Technology/Electronics/Signal+Integrity/ANSYS+HFSS>
- [11] <https://www.sparkfun.com/products/10128>
- [12] http://www.nxp.com/products/identification-and-security/smart-label-and-tag-ics/iccode:MC_42024